

Engineered CuInSe_xS_{2-x} Quantum Dots for Sensitized Solar Cells

Hunter McDaniel,^{*,†} Nobuhiro Fuke,^{*,§} Jeffrey M. Pietryga, and Victor Klimov^{*}

[†]Center for Advanced Solar Photophysics, Department of Chemistry, Los Alamos National Laboratory, Los Alamos, New Mexico 87545, USA

[§]Materials & Energy Technology Laboratories, Corporate Research and Development Group, Sharp Corporation, 282-1 Hajikami, Katsuragi, Nara 639-2198, Japan

^{*}AUTHOR EMAIL ADDRESSES: hunter@lanl.gov; fuke.nobuhiro@sharp.co.jp; klimov@lanl.gov

Supporting Information

Additional experimental Details

General synthesis considerations

Reactions were carried out in a standard Schlenk line under argon atmosphere. Technical grade oleylamine (70%), technical grade trioctylphosphine (TOP) (90%), technical grade 1-octadecene (90%), technical grade oleic acid (90%), 1-dodecanethiol (98%), tert-butylamine (98%), CdO (99.5%), Se powder (99.99%), S powder (99.5%), indium acetate (In(III)(Ac)₃) (99.99%), copper iodide (Cu(I)I) (99.5%), anhydrous methanol (99.8%), anhydrous acetone (99.8%), anhydrous octane (99.9%), and anhydrous chloroform (99.9%) were obtained from Sigma Aldrich. Anhydrous sodium sulfide (Na₂S) was purchased from Alfa Aesar. Materials were used as received.

Characterization

Transmission Electron Microscopy (TEM)

Transmission electron microscopy (TEM) samples were prepared on Cu grids (obtained from Ted Pella) with a thin carbon film on a holey carbon support from a dilute solution of NCs in chloroform. TEM analysis was carried out with a JEOL 2010 TEM operating at 200 kV.

Scanning Electron Microscopy (SEM) and X-ray Dispersive Spectroscopy (EDX)

Scanning electron microscopy (SEM) samples were prepared by breaking a QDSSC anode in half, then the cross-section was analyzed using a Quanta 400 FEG from FEI Company operating at 10kV. The electron beam was scanned across the cross-section and the energy and the count of X-rays were analyzed to produce an EDX scan. Elemental analysis was conducted using Genesis EDX software

Absorption and Photoluminescence (PL) Spectroscopy

All optical measurements of QDs in solution were performed in either chloroform or octane using a quartz or optical glass cuvette. UV-vis absorption spectra were obtained with Agilent 8453 photodiode array spectrometer. Visible static PL was measured on a Horiba-Yvon Fluoromax 4 with 500 nm excitation. Time resolved PL was measured on the same Horiba-Yvon Fluoromax 4 with a pulsed 455 nm LED excitation. Near-IR PL measurements were performed under 808 nm diode laser excitation using a liquid N₂ cooled InSb detector with a grating monochromator. The excitation was mechanically chopped and the signal was enhanced with a lock-in amplifier.

Solar Cell Characterization

The EQE measurements were performed using QE/IPCE Measurement Kit equipped with 150 W Xe lamp (no. 6253, Newport) as a light source and Oriel Cornerstone monochromator. The light intensity was adjusted with a series of neutral density filters and monitored with a Newport optical power meter 1830C power meter with a calibrated Si power meter, Newport model 818 UV. The photocurrent generated by the device was measured using a Keithley 6517A electrometer. Communication between the instruments and the computer was facilitated via a GPIB interface and the instrument control and data processing were performed using software written locally in

Labview. Current voltage (I-V) measurements were performed using a Keithly 2400 SourceMeter as part of a model SC01 solar cell characterization system (software and hardware) built by PV Measurements. A class ABA solar simulator (AM 1.5), also built by PV Measurements, was calibrated using a Newport-certified single crystal Si solar cell, then was used to irradiate the QDSSCs during I-V measurement. The voltage was swept from -0.1V to 0.6V at 0.01 V/step with a 1s hold-time at each point prior to measurement. A square black mask (0.2209 cm^2) was attached to the solar cells to prevent irradiation by scattered light.

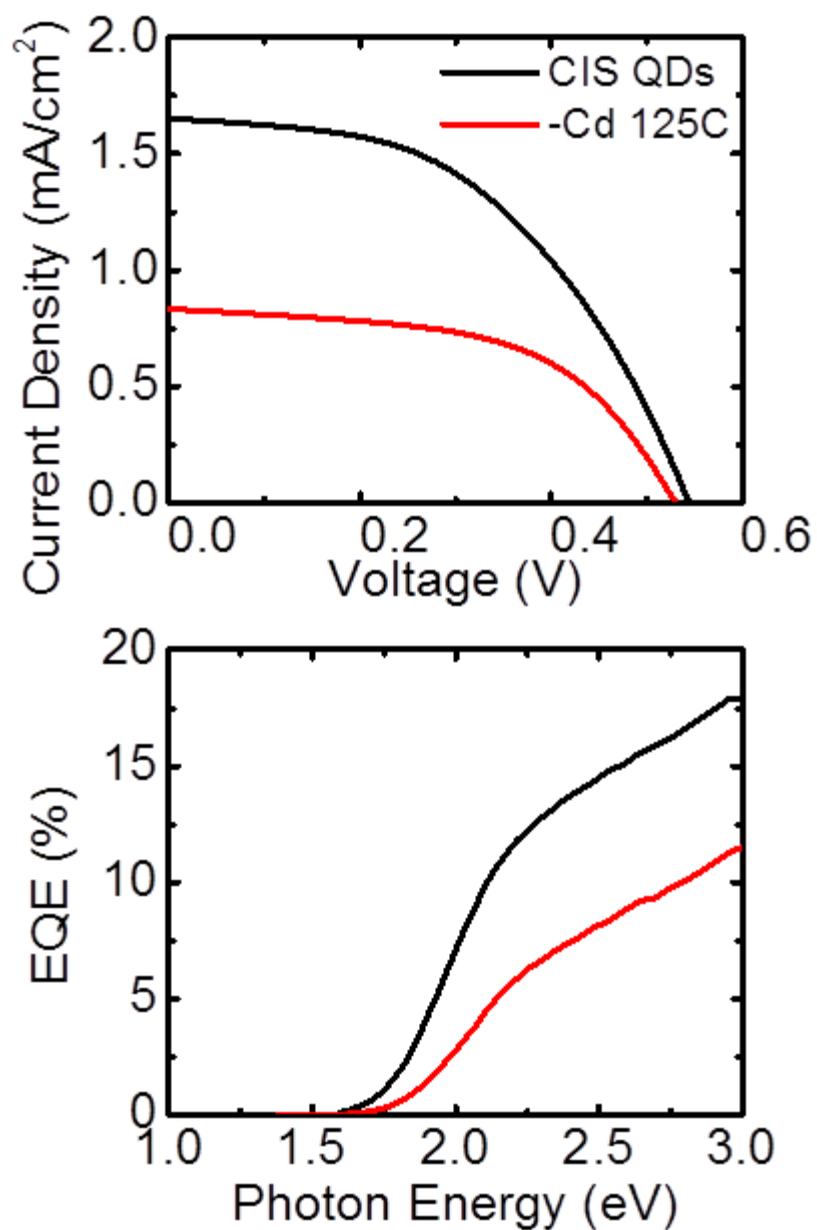


Figure S1: I-V (top) and EQE (bottom) data for QDSSCs made with CuInS₂ (CIS) QDs (no Se) without (black) and with (red) Cd-oleate treatment at 125 °C. The lower performance with the Cd treatment is primarily attributed to very poor QD loading in the film (*i.e.* lighter color for the Cd-treated QD-sensitized mp-TiO₂ film after sensitization).

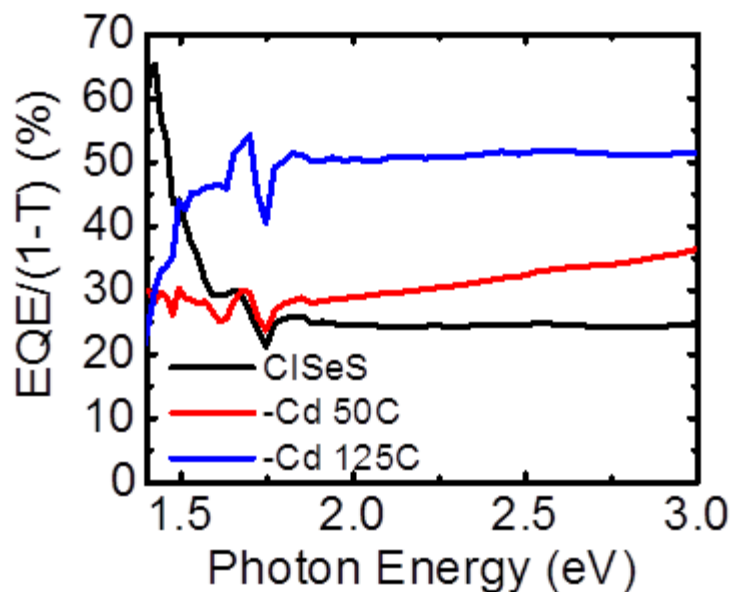


Figure S2: EQE/(1-T) compiled from the EQE and (1-T) data shown in Figure 3. EQE/(1-T) provides a lower limit for the internal quantum efficiency (IQE) of the devices.

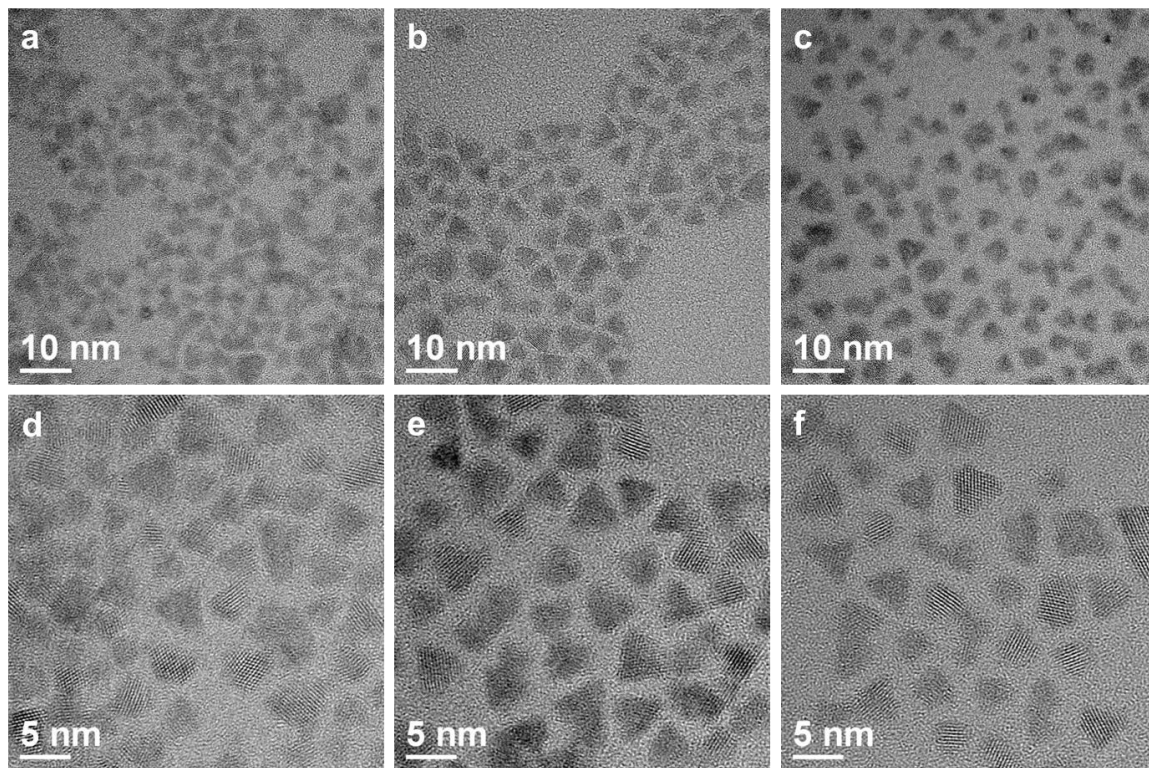


Figure S3: Low (a-c) and high (d-f) magnification TEM images of $\text{CuInSe}_{1.4}\text{S}_{0.6}$ QDs before cation exchange (a,d), after cation exchange at 50 °C (b, e), and after cation exchange at 125 °C (c, f). Size is measured from a vertex to the middle of the opposite edge of the triangular shapes for 30 QDs in each case; the average sizes were 4.23 nm (± 0.30 nm) before cation exchange, 4.13 nm (± 0.26 nm) after cation exchange at 50 °C, and 4.10 nm (± 0.27 nm) after cation exchange at 125 °C. The QDs shown are the same QDs characterized in Figure 1b, Figure 2, and Figure 3, although they have not been recapped.

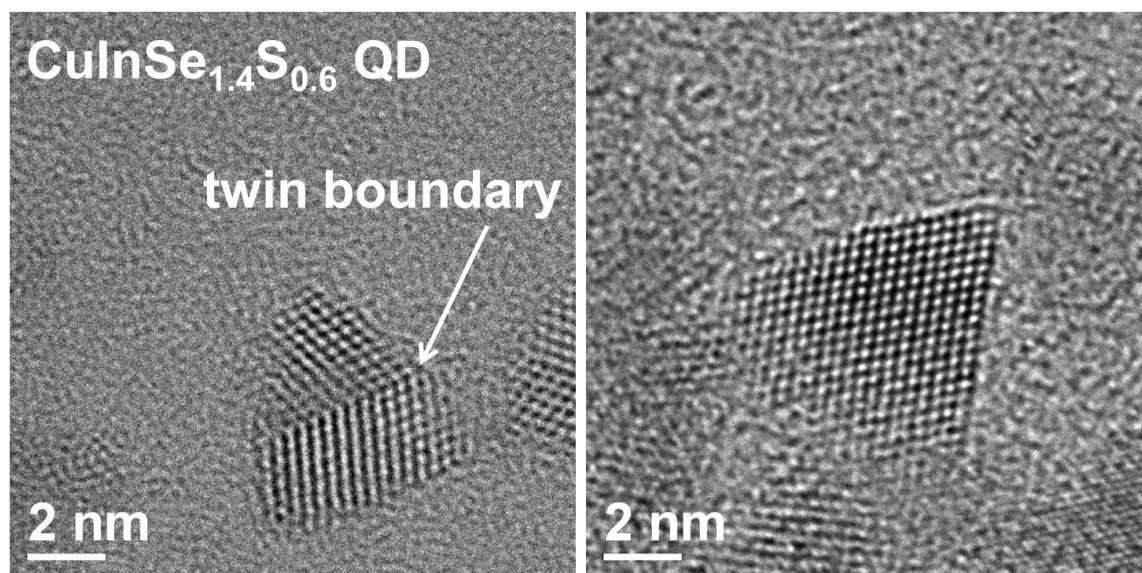


Figure S4: High resolution TEM images of larger than average CuInSe_{1.4}S_{0.6} QDs (no cation exchange). Aside from the occasional twin boundary (left), these QDs appear to have a homogeneous crystal structure with uniform lattice constants throughout.

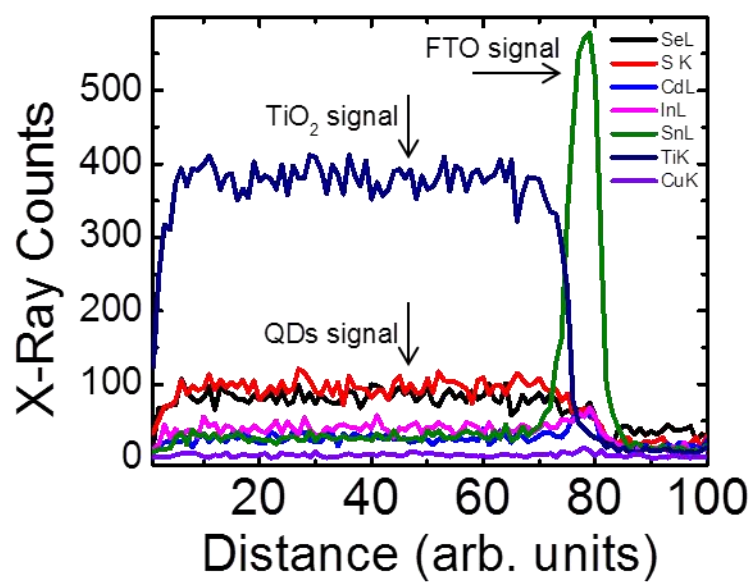
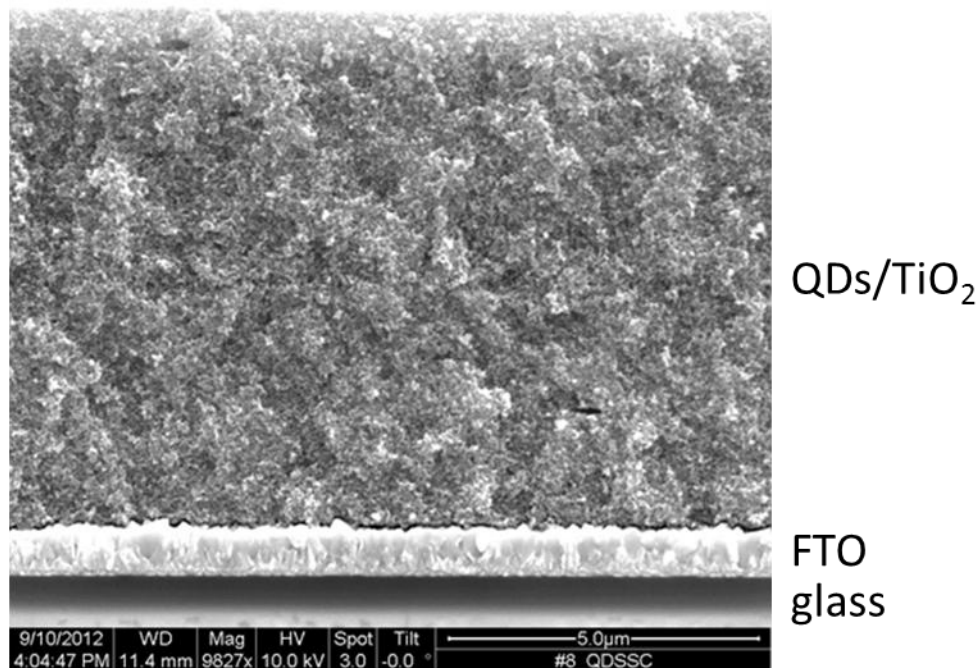


Figure S5. SEM cross section image of a sensitized film on FTO coated glass (top). Raw data of an EDX line scan of this cross section showing the even concentration of QDs throughout the mp-TiO₂ film.

Day 1	V_{oc} (V)	J_{sc} (mA/cm²)	FF	PCE (%)
ClSeS QDs	0.425	3.59	0.470	0.72
-Cd 50C	0.545	6.36	0.576	2.00
-Cd 125C	0.535	5.14	0.587	1.61
-Cd 50C DL	0.535	8.72	0.511	2.38

Day 4	V_{oc} (V)	J_{sc} (mA/cm²)	FF	PCE (%)
ClSeS QDs	0.115	0.34	0.257	0.01
-Cd 50C	0.535	6.78	0.573	2.08
-Cd 125C	0.545	6.21	0.572	1.94
-Cd 50C DL	0.545	9.42	0.489	2.51

Figure S6: Table of the photovoltaic properties of the I-V curves shown in Figures 3a and 3b.